Brief Communications

α-Synuclein Inhibits Intersynaptic Vesicle Mobility and Maintains Recycling-Pool Homeostasis

David Scott[1] **and Subhojit Roy**[1,2]

Departments of [1]Pathology and [2]Neurosciences, University of California, San Diego, La Jolla, California 92093

Although the presynaptic protein α-synuclein is a recognized player in neurodegeneration, its precise physiologic function(s) and/or role in human disease remains unclear. An emerging consensus from previous studies in lower-order systems is that α-synuclein interferes with vesicle-trafficking pathways; however putative neuronal correlates are unknown. Here we explore consequences of α-synuclein modulation in cultured mouse hippocampal neurons; coupling α-synuclein overexpression and knock-out model-systems with contemporary imaging paradigms. Our studies reveal an unexpected role of α-synuclein in attenuating the mobility of recycling pool (RP) vesicles between presynaptic boutons— called "superpool" trafficking—and also in maintaining the overall size of RPs at synapses. While an excess of α-synuclein led to smaller RPs and inhibited intersynaptic trafficking, an absence of α-synuclein triggered converse changes with larger RPs and enhanced intersynaptic trafficking. The data collectively suggest a model where α-synuclein maintains RP homeostasis by modulating intersynaptic vesicular dynamics, and provide a putative neuronal correlate of α-synuclein-induced impairments in vesicle-trafficking previously reported in lower-order systems.

Introduction

The small presynaptic protein α-synuclein plays a central role in several neurodegenerative diseases, collectively called "synucleinopathies." Despite considerable interest, neither the normal function(s) of α-synuclein, nor consequences of its overexpression are fully understood. Previous studies in lower-order systems have consistently shown that α-synuclein interferes with vesicle-trafficking pathways. This is best studied in the yeast, where the evidence is compelling. Expression of α-synuclein in yeast inhibits ER→Golgi trafficking (Outeiro and Lindquist, 2003; Cooper et al., 2006; Gitler et al., 2008; Soper et al., 2008) that can be rescued by genes that facilitate this pathway (Cooper et al., 2006; Soper et al., 2008). Vesicular α-synuclein accumulations—likely secondary to trafficking deficits—are also seen at an ultrastructural level (Gitler et al., 2008; Soper et al., 2008; Pranke et al., 2011), consistent with ER→Golgi trafficking impairments, and unbiased yeast genetic screens implicate trafficking-pathways as well (Willingham et al., 2003). Similar α-synuclein-induced phenotypes have been reported in non-neuronal/PC-12 cell-lines (Thayanidhi et al., 2010), *C. elegans* (Cooper et al., 2006; Gitler et al., 2008; Kuwahara et al., 2008; van Ham et al., 2008) and *Drosophila* (Cooper et al., 2006), collectively making a rather strong case that α-synuclein inhibits vesicle-trafficking pathways.

However, while deficits in secretory-trafficking pathways are important clues; in neurons, the vast majority of α-synuclein is not normally localized around the ER/Golgi, but is instead concentrated at distal presynapses. Thus we reason that putative neuronal α-synuclein-induced vesicle-trafficking deficits are likely to first manifest at/around synapses. Here we employ knock-out and overexpressing systems to evaluate effects of α-synuclein modulations on synapses. Our data suggest unexpected roles of α-synuclein in regulating synaptic vesicle trafficking and maintaining recycling pool (RP) homeostasis.

Materials and Methods

Cell culture, live imaging, FM4-64 experiments, and immunostaining

See Scott et al. (2010) for basic details. Briefly, cells from postnatal (P0–P1) mice were plated (30,000–60,000 cells/cm^2) and cultured to maturity [days *in vitro* (DIV) 17–21] before experimental manipulations. For transient FM4-64 loading, neurons were incubated in stimulation solution (containing, in mM: 5 HEPES, 90 NaCl, 1 $MgCl_2$, 2 $CaCl_2$, 10 glucose, and 47 KCl) containing 10–15 μM FM4-64 and NMDA-antagonists (50 μM DL-AP5, 20 μM CNQX) for 90 s; a protocol known to label functional RPs (Darcy et al., 2006; Gaffield and Betz, 2006). For field-stimulation experiments, neurons were placed in a chamber (EC-B-18—Chamlide EC) connected to an SD9-square-pulse stimulator (Grass Instruments) and imaged every 3 s. Resultant data were photobleach-corrected. α-Synuclein-null mice were obtained from Jackson Labs. For experiments involving paired wild-type (WT), +/−, and −/− littermates, identity of pups was confirmed by genotyping. All University of California, San Diego guidelines were followed. Experiments were repeated at least 2–3 times on separate culture-sets. C57BL/6 mouse pups of either sex were used.

Received Feb. 3, 2012; revised May 11, 2012; accepted June 4, 2012.

Author contributions: D.S. and S.R. designed research; D.S. and S.R. performed research; D.S. and S.R. analyzed data; S.R. wrote the paper.

This work was supported by grants from the Larry Hillblom Foundation, the Alzheimer's Association (NIRG-08-90769), the American Federation for Aging Research (AFAR), and NIH (Grants P50AG005131 and R01NS075233) to S.R. We thank Yong Tang and Utpal Das for help with genotyping, Edward Rockenstein and Eliezer Masliah for α-synuclein:GFP transgenic breeders, Steve Edland for statistical consultation, and Christina Sigurdson for helpful comments on the manuscript [all at University of California, San Diego (UCSD)].We also acknowledge the UCSD Neuroscience Microscopy Shared Facility Grant (P30 NS047101) for confocal FRAP imaging.

Correspondence should be addressed to Dr. Subhojit Roy, 312 MTF, 9500 Gilman Drive MC 0624, University of California, San Diego, CA 92093. E-mail: s1roy@ucsd.edu.

DOI:10.1523/JNEUROSCI.0535-12.2012

 0270-6474/12/3210129-07$15.00/0

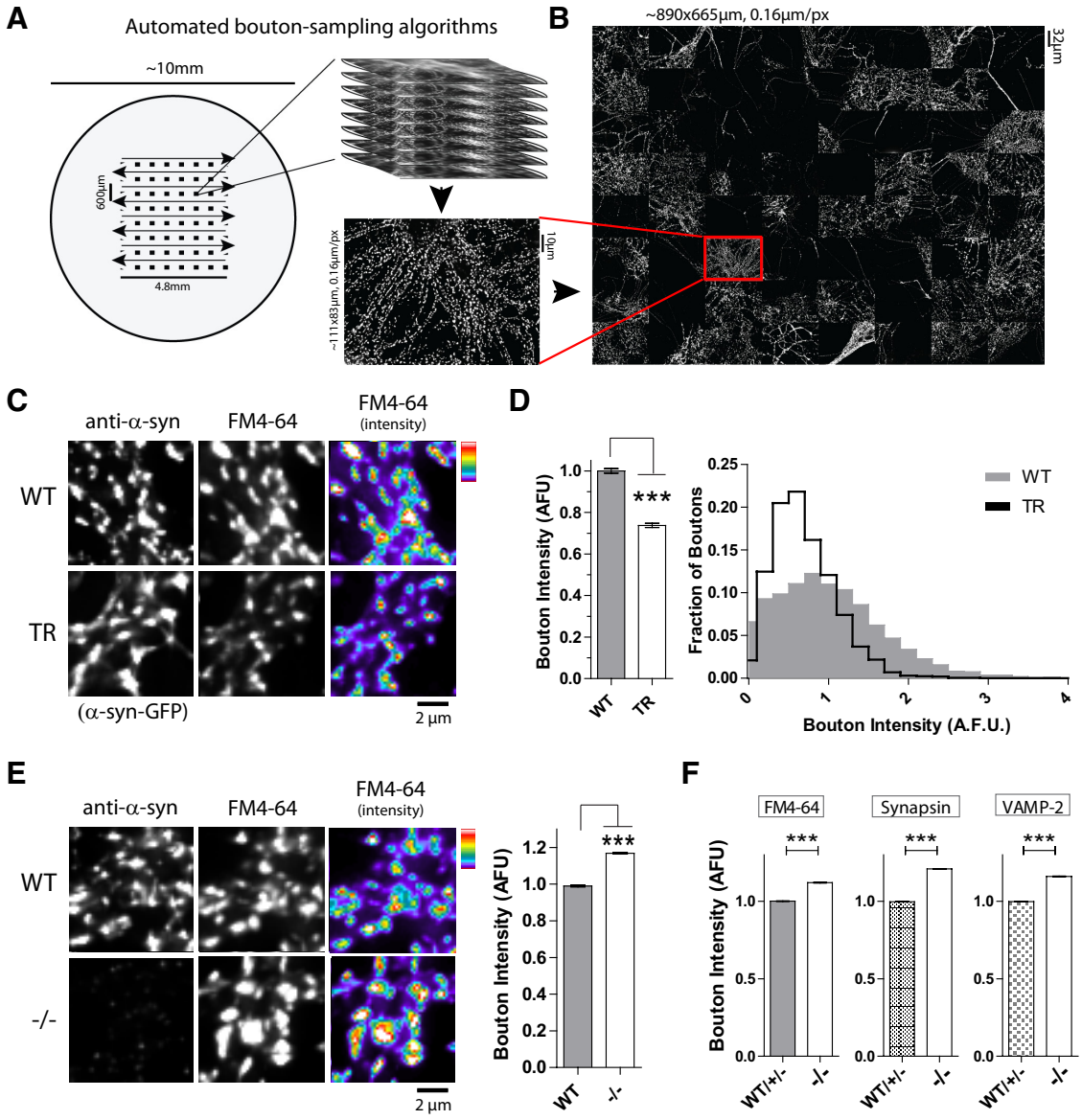

Figure 1. Converse effects of α-synuclein overexpression/absence on recycling pool size. ***A***, Automated bouton sampling algorithms. Boutons were sampled by placing virtual 8 × 8 grids on a coverslip (left, large circle represents coverslip; arrows indicate sampling trajectory) and serial *z*-stacks were obtained, resulting in the acquisition of 64 *z*-stacks distributed over a 4.8 × 4.8 mm area of a 10 mm coverslip (see Materials and Methods). ***B***, Maximum-intensity projections were computationally "stitched" into a montage (890.88 × 665.6 μm, resolution 0.16 μm/pixel) and analyzed. ***C***, Images of WT and α-synuclein transgenic (TR) neurons loaded with FM4-64. ***D***, Normalized average FM4-64 intensities in DIV 17–21 transgenic boutons (compared with WT) were 0.75 ± 0.01 ($N \sim 4000–6000$ boutons were examined for each group; $^{***}p < 0.0001$. ***E***, FM4-64-loading in α-synuclein $^{-/-}$ neurons. Note increased FM-dye loading, quantified on right (relative average intensities in −/− boutons were 1.168 ± 0.0043 mean ± SEM, $^{***}p < 0.0001$; $N \sim 9000/7000$ boutons examined in WT/−/− cultures processed in parallel). ***F***, Left to right, Relative average FM4-64/synapsin-1/VAMP-2 intensities in −/− boutons (compared with boutons from littermate paired WT/+/− mice) were 1.12 ± 0.0010; 1.21 ± 0.0019; and 1.16 ± 0.0017 respectively ($N \sim 25{,}000–50{,}000$ boutons/condition; $^{***}p < 0.0001$). Data from two sets of paired littermates were pooled for display, but were also independently significant.

Fluorescence recovery after photobleaching experiments

All fluorescence recovery after photobleaching (FRAP) experiments were performed on a Fluoview-1000 confocal microscope (Olympus). FM4-64-loaded, adjacent en-passant boutons (separated by < 7 μm; Darcy et al., 2006) were photobleached to 30 ± 1% (mean ± SEM) of the original fluorescence intensity by scanning with a 515 nm laser at 100% power for 5 s (2.0 μs/pixel). Images were corrected for photobleaching, and FRAP kinetics for experimental groups were statistically analyzed by paired *t* test and expressed as mean ± SEM. A *p* value of < 0.05 was considered significant.

Image analysis

Automated bouton sampling algorithms. These algorithms automated the imaging process, sampled large areas, and significantly scaled up sample size. Regularly spaced 6 × 6 (or 8 × 8) field grids (696 × 520 pixels/grid) were distributed evenly over each coverslip (Fig. 1). *Z*-series images were acquired from each grid (36/64 *z*-series stacks for each coverslip) and deconvolved (Huygens). An auto-focusing algorithm facilitated rapid search for an optimal focal plane for each microscopic field while minimizing latent exposure of the field to incident light before acquisition. All image sampling and focusing algorithms were implemented as scripts for use within MetaMorph.

Synaptic colocalization algorithms. Image acquisition, deconvolution and colocalization-algorithms were similar to our previously published protocols (Scott et al., 2010). For retrospective correlation experiments, FM4-64+ boutons were imaged live and cultures were fixed/stained for mouse presynaptic proteins. Images were retrospectively aligned, and FM4-64/synaptic-protein intensities were quantified. Fidelity of the datasets was cross-checked with extensive manual sampling. For bouton-correlation experiments, some paired intensity measurements were square root transformed, and expressed as a correlation coefficient (Pearson's).

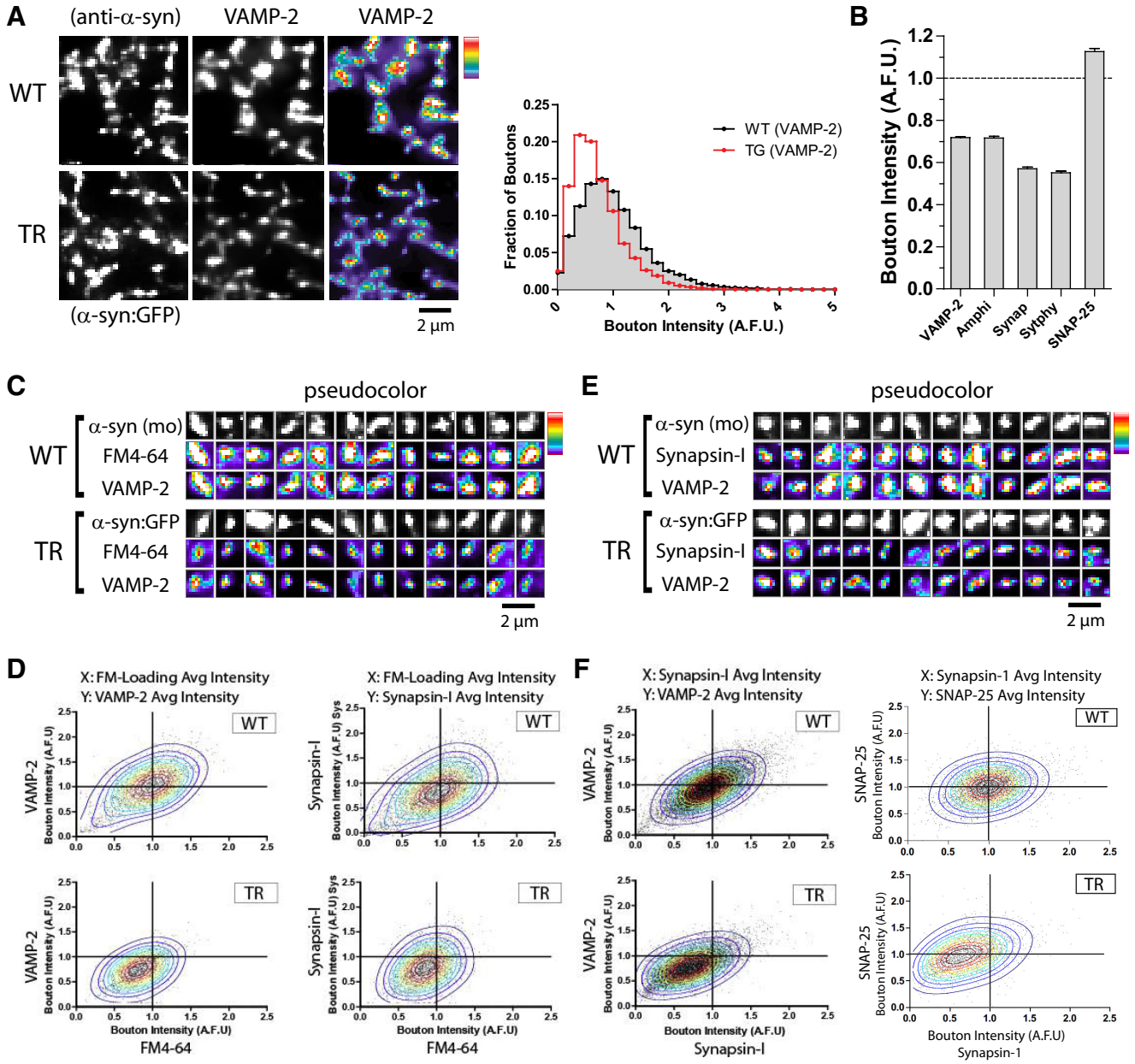

Figure 2. Diminished presynaptic protein levels in DIV 17–21 α-synuclein overexpressing boutons correlate with reduced recycling pools. ***A***, ***B***, Neurons overexpressing α-syn:GFP were fixed and stained with antibodies to endogenous mouse presynaptic proteins. Relative average fluorescence intensities of VAMP-2, amphiphysin, synapsin-1, synaptophysin and SNAP-25 in transgenic boutons (compared with controls) were 0.69 ± 0.007, 0.7 ± 0.008, 0.57 ± 0.007, 0.55 ± 0.008 and 1.12 ± 0.01 respectively, mean ± SEM, $p < 0.0001$, for all proteins, unpaired *t* test; $N \sim 5000 - 8000$ boutons/group. ***C***, Retrospective immunostaining (bouton-crops) of mouse presynaptic proteins in FM4-64-loaded boutons from WT and TR mice (see Materials and Methods). Note that boutons with low FM4-64 levels also have lower VAMP-2/synapsin-1 levels. ***D***, FM4-64 and VAMP-2/synapsin-1 average-intensities were correlated in WT neurons (correlation coefficient $r = 0.66/0.61$ for VAMP-2/synapsin-1 respectively), with negative X/Y mean-shifts in TR neurons, suggesting corresponding diminutions of both presynaptic members (compare X/Y-distributions in WT-top/TR-bottom graphs). ***E***, Representative immunostaining (bouton-crops) of WT or TR neurons with synapsin-1/VAMP-2. ***F***, Note corresponding X/Y mean-shifts in the TR boutons stained with synapsin-1/VAMP-2 (left-panels); but lack of Y mean-shift in synapsin-1/SNAP-25 correlations (right panels; see Materials and Methods).

Contour-plots were calculated using the 2-D kernel density estimation function supplied with the MCLUST package for R. Experimental groups were statistically analyzed using a nonparametric *t* test and expressed as mean ± SEM; a *p* value of < 0.05 was considered significant.

"FM4-64-Flux" analyses. Algorithms were developed in Matlab/MetaMorph. (1) Movies (120 s) of FM4-64-loaded boutons/intervening axons were acquired (2 Hz), corrected for photobleaching and background subtracted. (2) Flux was calculated as absolute change in intensity/pixel for each successive time-point by subtracting consecutive frames in a movie. This is represented as $[I(t_n) - I(t_{n-1})]$ where *I* is the absolute fluorescence intensity of each pixel, and *t* represents a given time-point. Resulting image-stacks were noise-corrected (Dussault and Hoess, 2004). (3) Eight to 12 pixel polylines were placed in axonal regions between FM4-64-positive boutons, and 2-D noise-corrected kymographs were generated. Pixel-intensities in kymographs were averaged and represented graphically as "average FM4-64-flux."

Results

Quantitative model-systems for evaluating α-synuclein biology

Three types of cultured hippocampal neurons were used in this study—neurons expressing WT α-synuclein, neurons lacking α-synuclein (from α-synuclein-null mice), and neurons overexpressing α-synuclein. Briefly, dissociated hippocampal neurons were obtained from mice overexpressing human α-synuclein

tagged to GFP (α-syn:GFP)—or lacking α-synuclein altogether (α-syn $^{-/-}$), and all experiments were performed in neurons cultured for 17–21 DIV. WT/+/− littermates were used as paired controls. There is an approximately twofold higher level of α-synuclein in DIV 17–21 α-syn:GFP neurons, with no detectable synaptic losses (Scott et al., 2010; see also Unni et al., 2010). This model-system offers several advantages. The α-synuclein-positive boutons can be visualized directly (by their native GFP-fluorescence), and the system is amenable to live-cell experiments. Moreover, large numbers of boutons can be analyzed (several thousand per experiment—see below) offering significant methodological advantages and statistical power over strategies using transient transfections. Upgrades to our previous protocols now allow us to evaluate considerably larger numbers of boutons in a relatively unbiased manner (Fig. 1*A*; Materials and Methods), minimizing the impact of intrinsic local variations in synaptic quantitation.

Converse changes in recycling pool size in neurons from α-synuclein overexpressing and null mice

Working with α-synuclein overexpressing model-systems, we and others previously reported reduced presynaptic uptake of the styryl dye FM4-64—a marker of functional RPs (Nemani et al., 2010; Scott et al., 2010). The extent of these diminutions, as well as the heterogeneity among individual synapses is shown in Figure 1, *C* and *D*. We used our bouton-sampling algorithms to compare RPs in neurons from α-synuclein-null mice (Abeliovich et al., 2000) with WT mice—processing cultures in parallel. Surprisingly, average FM4-64 intensities were significantly greater in α-synuclein $^{-/-}$ boutons (Fig. 1*E*). We also repeated these experiments in neurons from littermate-paired mice containing or lacking endogenous α-synuclein (WT/+/− and −/− respectively). Average intensities of both FM-dye uptake (Fig. 1*F*, left) and endogenous presynaptic protein levels were higher in −/− neurons (Fig. 1*F*, middle and right); unlike overexpressing neurons (see below).

Previously, we reported reduced presynaptic protein levels in α-synuclein overexpressing boutons (Scott et al., 2010). Using A53T-mutant α-synuclein mice, Lim and colleagues also found similar diminutions in vesicular presynaptic proteins *in vivo*, but with relative preservation of t-SNARE components (Lim et al., 2011). Revisiting the issue, we found that while levels of several membranous presynaptic proteins are diminished in α-synuclein overexpressing boutons, levels of the t-SNARE protein SNAP-25 were actually higher than littermate-controls (Fig. 2*A*,*B*; see also Burré et al., 2010; Garcia-Reitböck et al., 2010). Notably, we also repeated these experiments in neurons from an identical mouse model that lacks the GFP-tag (PDGF promoter-human-α-synuclein mice) with similar results (data not shown)—indicating that diminutions are independent of the GFP-tag. Hence α-synuclein-induced diminutions in presynaptic protein levels are likely a bona fide observation.

What is the basis for these diminutions? Since presynaptic proteins associate with synaptic vesicles (either integrally or peripherally), we asked whether such diminutions correlated with reduced RPs. WT/transgenic boutons were loaded with FM4-64, imaged, then fixed and stained the with mouse VAMP-2/synapsin-1 antibodies; retrospectively comparing VAMP-2/synapsin-1 fluorescence with corresponding FM4-64-intensities (see Materials and Methods). Bouton-crops (Fig. 2*C*) highlight correlated diminutions in FM4-64 and endogenous presynaptic

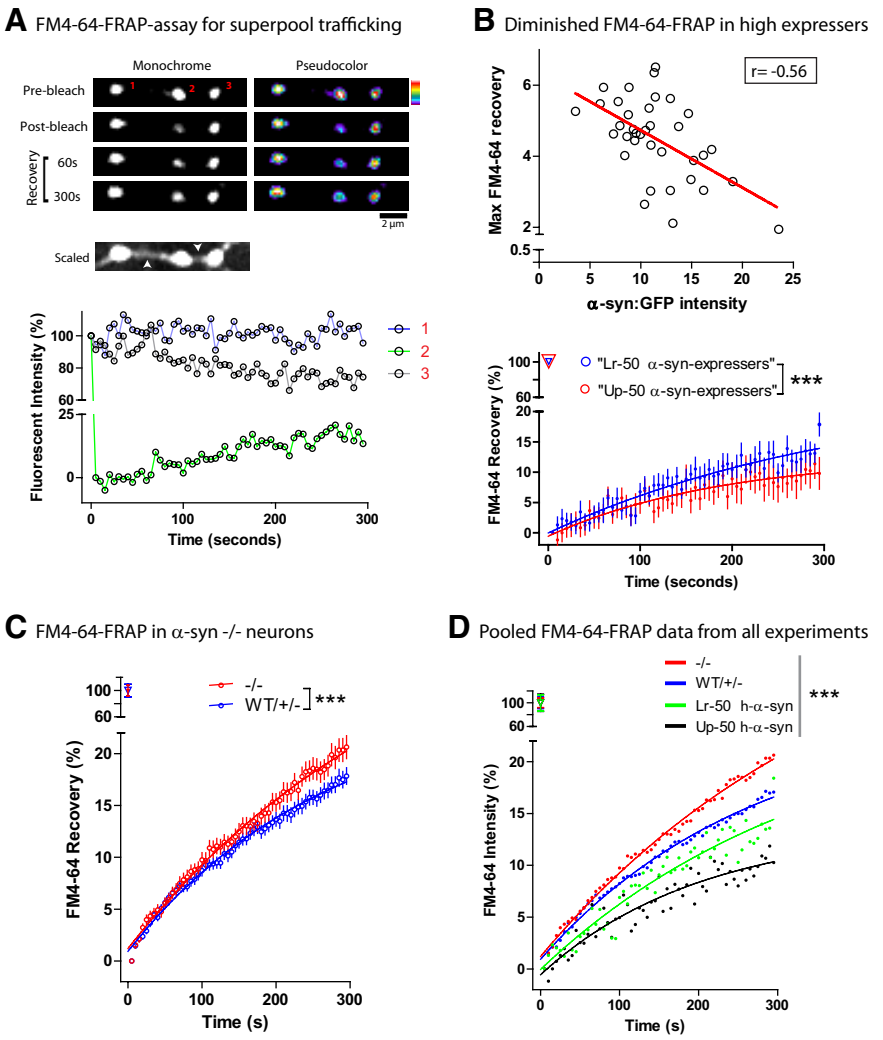

Figure 3. Converse effects of α-synuclein overexpression/absence on recycling pool kinetics. ***A***, DIV 17–21 transgenic (or WT) boutons were loaded with FM4-64, a string of boutons were selected (#1–3, "pre-bleach"), and a single bouton (#2) was selectively photobleached ("post-bleach"). Note recovery of fluorescence over time in the grayscale (left) and pseudocolor (right) images. Scaled image below shows axon continuity (arrowheads). Variations in intensities of the three boutons over time are graphically represented below. Note partial recovery of FM4-64 in the bleached bouton, reflecting exchange between boutons (see Results). ***B***, Top, Maximum FM4-64 recovery inversely correlated with α-syn:GFP intensities in the same boutons ($r = 0.56$; $p < 0.0001$). Bottom, Kinetics of FM4-64-recovery was also significantly diminished in the upper 50 th percentile of overexpressers (see Results). $N \sim 40$ boutons/group, $^{***}p < 0.0001$. ***C***, Conversely, the rate of FM4-64 FRAP recovery was significantly faster in DIV 17–21 α-synuclein $^{-/-}$ neurons, compared with their WT/+/− littermates (containing α-synuclein). ($N \sim 60$–90 boutons/group, $^{***}p < 0.0001$). ***D***, Pooled FM4-64-FRAP data from all experiments show an incremental diminution of FM4-64 mobility upon increasing α-synuclein dosage. $^{***}p < 0.0001$, one-way ANOVA.

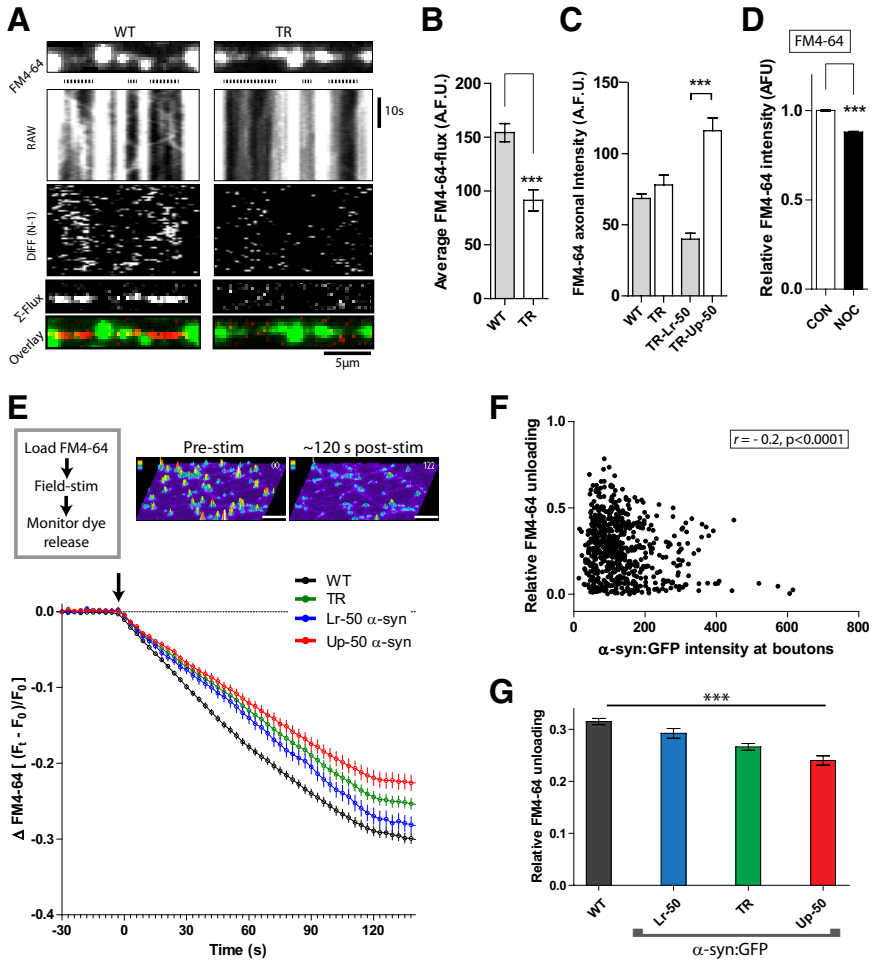

Figure 4. Direct assay of the superpool and FM4-64 exocytosis in α-syn:GFP-expressing neurons. ***A***, Top to bottom, (1) Images of FM4-64-loaded WT/TR boutons; (2) raw kymographs showing trafficking of FM4-64-labeled vesicles (diagonal lines) between stationary boutons (vertical lines); (3) difference [DIFF ($N - 1$) kymographs showing inter-boutonic fluctuations of fluorescence intensities; (4) cumulative FM4-64 flux (Σ-flux, "flattened" image); (5) overlay of FM4-64/Σ-flux. ***B***, The cumulative FM4-64 flux was significantly lower in TR neurons, compared with WT littermates [91.36 ± 9.83 arbitrary fluorescence units (AFU) and 154.3 ± 8.41 AFU, respectively; mean ± SEM, ***$p < 0.0001$; $N = 80–120$ boutons/group]. ***C***, The cumulative FM4-64 flux was significantly lower in TR neurons, compared with WT littermates (91.36 ± 9.83 AFU and 154.3 ± 8.41 AFU, respectively; mean ± SEM, ***$p < 0.0001$; $N = 80–120$ axonal-segments/group). ***D***, FM4-64-loading was lower in Nocodazole-treated neurons (0.88 ± 0.0044, mean ± SEM, N ~20,000–30,000 boutons/group, ***$p < 0.0001$). ***E***, WT/α-syn:GFP boutons were loaded with FM4-64 (see Materials and Methods), and stimulation-dependent (arrow) release of FM-dye from boutons was monitored (1200 action potentials at 10 Hz; 60 mA, 1 ms). Change in FM4-64-fluorescence (ΔF) was quantified as [fluorescence at each time-point (F_t) − initial fluorescence (F_0, average of all prestimulation frames)]/F_0 (Waites et al., 2011); note that not all K^+-loaded boutons can be unloaded by these methods (see also Waites et al., 2011). Kinetics of FM4-64 decay (Materials and Methods) was slower in α-syn:GFP-expressing boutons, and was greatly attenuated in the highest α-syn:GFP expressers (Up-50, see Results). $N = 1363/635$ boutons, WT/TR. ***F***, Scatter plots of α-syn:GFP intensities and the extent of FM4-64 unloading (average residual fluorescence over the last 5-frames of the decay-curves). Note that FM4-64-unloading is attenuated in high α-syn:GFP expressers. ***G***, Bar graphs comparing FM4-64 unloading (as above) between various groups (***$p < 0.0001$, one-way ANOVA).

proteins; quantitatively depicted in Figure 2*D*. Moreover, corresponding diminutions in synapsin-1/VAMP-2 levels were seen in the same α-syn:GFP overexpressing boutons (Fig. 2*F*, left; but not with synapsin-1/SNAP-25, Fig. 2*F*, right—see above). Though a diminished RP level is likely responsible for the "reduced presynaptic-protein" phenotype, effects of other processes (e.g., reduced axonal transport) cannot be excluded and will require more focused experiments.

Converse changes in recycling pool trafficking in neurons from α-synuclein overexpressing and null mice

Collectively, the above data suggest that α-synuclein may be involved in maintaining RPs at steady-state levels. RP levels are maintained at equilibrium by replenishment from local and imported sources (for review, see Denker and Rizzoli, 2010)—the former by endocytic retrieval of recycling vesicles within individual boutons post-exocytosis, and the latter via refilling of RPs via trafficking vesicles. Specifically, recent studies have shown that RP vesicles are continuously exchanged within adjacent boutons in resting neurons—a phenomenon dubbed "superpool" trafficking (Krueger et al., 2003; Darcy et al., 2006; Staras et al., 2010; Herzog et al., 2011; Ratnayaka et al., 2011).

Given the known effects of α-synuclein on vesicle-trafficking in lower-order systems, we asked whether superpool-trafficking was altered in neurons overexpressing/lacking α-synuclein. Toward this we first used an "FM4-64-FRAP assay" that reports the exchange of RP vesicles between boutons (Darcy et al., 2006; Staras et al., 2010). Boutons were loaded with FM-dyes to label RPs, fluorescence within a single bouton is photobleached, and FM-dye recovery within the bleached bouton was monitored. As recovery is contingent upon movement of unbleached fluorescent molecules from adjacent boutons into the bleached bouton (Lippincott-Schwartz et al., 2003), the extent of FM-dye recovery reports the overall mobility of the superpool (Fig. 3*A*). In FM4-64-FRAP experiments with boutons containing α-syn:GFP, we found a significant negative correlation between the maximum extent of FM4-64 recovery and the intensity of α-syn:GFP within the same bouton (Fig. 3*B*, top), suggesting that α-synuclein may have an inhibitory effect on intersynaptic vesicle-trafficking. Furthermore, kinetics of FM4-64 recovery were significantly slower in high α-syn:GFP overexpressers—quantitatively defined as simply the upper 50th percentile of the average GFP intensity-range across all boutons (Fig. 3*B*, bottom).

Intriguingly, similar FM4-64-FRAP experiments in α-synuclein $^{-/-}$ neurons revealed converse changes, where the extent of FM4-64 recovery was higher in neurons from α-synuclein $^{-/-}$ mice, compared with their WT/+/− littermates (Fig. 3*C*). Remarkably, when we compare all our FM4-64-FRAP data from WT, +/−, and −/− DIV 17–21 neurons, there appears to be a dose-dependent influence of α-synuclein on FM4-64 recovery (Fig. 3*D*). Specifically, the extent of FM-dye recovery is lowest in boutons containing the highest levels of α-synuclein (Up-50 h-α-syn in Fig. 3*D*); whereas the most rapid FM-dye recovery occurs in the α-synuclein $^{-/-}$ boutons, suggesting that α-synuclein may have a role in "fine-tuning" this trafficking process.

Direct visualization of superpool and FM4-64 exocytosis

Though the trafficking of FM4-64 vesicles between boutons is obvious in videos, the mobile particles are heterogeneous and vary greatly in intensities, making manual tracking/quantifica-

tion difficult (see also Darcy et al., 2006)—prompting us to develop an "FM-flux" assay to directly monitor the superpool. Transgenic neurons were loaded with FM4-64, both α-syn:GFP and FM4-64 fluorescence was simultaneously imaged, and successive frames in a movie were subtracted to eliminate stationary fluorescence (including synaptic fluorescence that was largely stationary over these short time-scales). These methods robustly highlighted the flux of FM4-64-particles in inter-boutonic axons (Fig. 4*A*). Significant reductions of FM4-64-flux were seen in α-synuclein overexpressing neurons (Fig. 4*B*), arguing that α-synuclein induces a specific trafficking-deficit. Furthermore, such inhibitions resulted in stalling of FM4-64 particles in axons, leading to an increase in cumulative inter-boutonic axonal FM4-64-fluorescence from "un-subtracted" movies (Fig. 4*C*). We also saw instances where α-syn:GFP and FM4-64 particles were cotransported in inter-boutonic axons (48/144 particles, ~33% were positive for both) suggesting physical associations of α-synuclein with trafficking synaptic vesicles. Finally, interruptions of vesicle-trafficking using the microtubule-depolymerizing drug nocodazole also reduced RP levels (Fig. 4*D*), arguing that an inhibition of trafficking/transport could result in diminished RPs.

We also monitored stimulus-dependent FM-dye exocytosis in WT and α-syn:GFP+ boutons. Increased α-synuclein levels led to reductions in exocytosis, and the data suggest a dose-dependent effect of α-synuclein on release-kinetics (Fig. 4*E–G*).

Discussion

Exploring the cell biology of α-synuclein in overexpressing and knock-out neurons, we found unexpected roles of α-synuclein in modulating the size and dynamics of synaptic vesicle pools. Specifically, α-synuclein inhibits the intersynaptic vesicle-trafficking and manipulating α-synuclein levels influences the overall size of recycling pools (RPs) at synapses, as well as their release properties. Collectively, the data suggest that α-synuclein maintains vesicle-pools within boutons at equilibrium by modulating/regulating vesicle-motility. This view does not necessarily exclude other possibilities—for instance effects of α-synuclein on local endocytosis and/or membrane-curvatures (Pranke et al., 2011)—that may also be a part of (or lead to) the spectrum of disrupted vesicle-trafficking. However, our data cannot conclusively link the α-synuclein-induced superpool deficits to changes in RP-size, and independent effects of α-synuclein on these two variables cannot be ruled out.

α-Synuclein as a regulator of recycling pool homeostasis and neurotransmitter release

Normal synaptic transmission depends upon a pool of vesicles that recycle with the presynaptic plasma-membrane and release their content (neurotransmitters) into the synaptic cleft (for review, see Denker and Rizzoli, 2010). Thus, the RP is a key player in neurotransmitter release, and release-probability (p_r) at synapses is known to correlate with RP-size (Murthy et al., 1997). Our FM-dye uptake experiments in mice overexpressing/lacking α-synuclein (Fig. 1) suggest that α-synuclein may have a role in regulating the overall size of RPs; and our FM-dye release experiments (Fig. 4*E–G*) suggest α-synuclein-dependent diminutions in release-kinetics. The notion that α-synuclein is a negative regulator of exocytosis is also supported by recent studies showing exaggerated synaptic responses in αβγ-synuclein-knock-out mice (Greten-Harrison et al., 2010; Anwar et al., 2010)—though this view has been challenged (Burré et al., 2010).

α-Synuclein as an inhibitor of superpool trafficking

Neuronal correlates of α-synuclein-induced vesicle-trafficking deficits found in lower-order systems have been mysterious. Using FRAP as well as direct flux-imaging assays, our data show that excessive α-synuclein inhibits the trafficking of synaptic vesicles between boutons—the superpool. The superpool is a large repository of synaptic vesicles (including recycling vesicles) that spans several boutons and is continuously exchanged among them in the resting state (Darcy et al., 2006; Staras et al., 2010; Herzog et al., 2011). Estimates suggest that this pool may be >100-fold larger in size than the RP at an individual bouton, and superpool-vesicles are recruited into boutons, where they appear to undergo exocytosis (Staras et al., 2010; Ratnayaka et al., 2011)—suggesting a dynamic repository of vesicles that can be recruited into individual synapses. Emerging evidence extends the superpool to recycling as well as resting vesicle-pools, and also implicates another peripheral presynaptic protein (synapsin) in regulating superpool-dynamics (Orenbuch et al., 2012). Given the enormous distances that may exist between the soma and a presynaptic bouton, the existence of such a process is also conceptually appealing. At this time, the precise molecular details underlying α-synuclein-mediated attenuation of superpool-trafficking are unclear. Further studies are also needed to unequivocally establish a mechanistic relationship between superpool-trafficking and RP-size.

References

Abeliovich A, Schmitz Y, Fariñas I, Choi-Lundberg D, Ho WH, Castillo PE, Shinsky N, Verdugo JM, Armanini M, Ryan A, Hynes M, Phillips H, Sulzer D, Rosenthal A (2000) Mice lacking alpha-synuclein display functional deficits in the nigrostriatal dopamine system. Neuron 25:239–252.

Anwar S, Peters O, Millership S, Ninkina N, Doig N, Connor-Robson N, Threlfell S, Kooner G, Deacon RM, Bannerman DM, Bolam JP, Chandra SS, Cragg SJ, Wade-Martins R, Buchman VL (2011) Functional alterations to the nigrostriatal system in mice lacking all three members of the synuclein family. J Neurosci 31:7264–7274.

Burré J, Sharma M, Tsetsenis T, Buchman V, Etherton MR, Südhof TC (2010) Alpha-synuclein promotes SNARE-complex assembly in vivo and in vitro. Science 329:1663–1667.

Cooper AA, Gitler AD, Cashikar A, Haynes CM, Hill KJ, Bhullar B, Liu K, Xu K, Strathearn KE, Liu F, Cao S, Caldwell KA, Caldwell GA, Marsischky G, Kolodner RD, Labaer J, Rochet JC, Bonini NM, Lindquist S (2006) Alpha-synuclein blocks ER-Golgi traffic and Rab1 rescues neuron loss in Parkinson's models. Science 313:324–328.

Darcy KJ, Staras K, Collinson LM, Goda Y (2006) Constitutive sharing of recycling synaptic vesicles between presynaptic boutons. Nat Neurosci 9:315–321.

Denker A, Rizzoli SO (2010) Synaptic vesicle pools: an update. Front Synaptic Neurosci 2:135.

Dussault D, Hoess P (2004) Noise performance comparison of ICCD with CCD and EMCCD cameras. Proc SPIE 5563:195–206.

Gaffield MA, Betz WJ (2006) Imaging synaptic vesicle exocytosis and endocytosis with FM dyes. Nat Protoc 1:2916–2921.

Garcia-Reitböck P, Anichtchik O, Bellucci A, Iovino M, Ballini C, Fineberg E, Ghetti B, Della Corte L, Spano P, Tofaris GK, Goedert M, Spillantini MG (2010) SNARE protein redistribution and synaptic failure in a transgenic mouse model of Parkinson's disease. Brain 133:2032–2044.

Gitler AD, Bevis BJ, Shorter J, Strathearn KE, Hamamichi S, Su LJ, Caldwell KA, Caldwell GA, Rochet JC, McCaffery JM, Barlowe C, Lindquist S (2008) The Parkinson's disease protein alpha-synuclein disrupts cellular Rab homeostasis. Proc Natl Acad Sci U S A 105:145–150.

Greten-Harrison B, Polydoro M, Morimoto-Tomita M, Diao L, Williams AM, Nie EH, Makani S, Tian N, Castillo PE, Buchman VL, Chandra SS (2010) αβγ-Synuclein triple knockout mice reveal age-dependent neuronal dysfunction. Proc Natl Acad Sci U S A 107:19573–19578.

Herzog E, Nadrigny F, Silm K, Biesemann C, Helling I, Bersot T, Steffens H,

Schwartzmann R, Nägerl UV, El Mestikawy S, Rhee J, Kirchhoff F, Brose N (2011) In vivo imaging of intersynaptic vesicle exchange using VGLUT1 Venus knock-in mice. J Neurosci 31:15544–15559.

Krueger SR, Kolar A, Fitzsimonds RM (2003) The presynaptic release apparatus is functional in the absence of dendritic contact and highly mobile within isolated axons. Neuron 40:945–957.

Kuwahara T, Koyama A, Koyama S, Yoshina S, Ren CH, Kato T, Mitani S, Iwatsubo T (2008) A systematic RNAi screen reveals involvement of endocytic pathway in neuronal dysfunction in alpha-synuclein transgenic *C. elegans*. Hum Mol Genet 17:2997–3009.

Lim Y, Kehm VM, Lee EB, Soper JH, Li C, Trojanowski JQ, Lee VM (2011) α-Syn suppression reverses synaptic and memory defects in a mouse model of dementia with Lewy bodies. J Neurosci 31:10076–10087.

Lippincott-Schwartz J, Altan-Bonnet N, Patterson GH (2003) Photobleaching and photoactivation: following protein dynamics in living cells. Nat Cell Biol Suppl:S7–S14.

Murthy VN, Sejnowski TJ, Stevens CF (1997) Heterogeneous release properties of visualized individual hippocampal synapses. Neuron 18:599–612.

Nemani VM, Lu W, Berge V, Nakamura K, Onoa B, Lee MK, Chaudhry FA, Nicoll RA, Edwards RH (2010) Increased expression of alpha-synuclein reduces neurotransmitter release by inhibiting synaptic vesicle reclustering after endocytosis. Neuron 65:66–79.

Orenbuch A, Shalev L, Marra V, Sinai I, Lavy Y, Kahn J, Burden JJ, Staras K, Gitler D (2012) Synapsin selectively controls the mobility of resting pool vesicles at hippocampal terminals. J Neurosci 32:3969–3980.

Outeiro TF, Lindquist S (2003) Yeast cells provide insight into alpha-synuclein biology and pathobiology. Science 302:1772–1775.

Pranke IM, Morello V, Bigay J, Gibson K, Verbavatz JM, Antonny B, Jackson CL (2011) {alpha}-Synuclein and ALPS motifs are membrane curvature sensors whose contrasting chemistry mediates selective vesicle binding. J Cell Biol 194:89–103.

Ratnayaka A, Marra V, Branco T, Staras K (2011) Extrasynaptic vesicle recycling in mature hippocampal neurons. Nat Commun 2:531. doi:10.1038/ncomms1534.

Scott DA, Tabarean I, Tang Y, Cartier A, Masliah E, Roy S (2010) A pathologic cascade leading to synaptic dysfunction in alpha-synuclein-induced neurodegeneration. J Neurosci 30:8083–8095.

Soper JH, Roy S, Stieber A, Lee E, Wilson RB, Trojanowski JQ, Burd CG, Lee VM (2008) {alpha}-Synuclein-induced aggregation of cytoplasmic vesicles in *Saccharomyces cerevisiae*. Mol Biol Cell 19:1093–1103.

Staras K, Branco T, Burden JJ, Pozo K, Darcy K, Marra V, Ratnayaka A, Goda Y (2010) A vesicle superpool spans multiple presynaptic terminals in hippocampal neurons. Neuron 66:37–44.

Thayanidhi N, Helm JR, Nycz DC, Bentley M, Liang Y, Hay JC (2010) Alpha-synuclein delays endoplasmic reticulum (ER)-to-Golgi transport in mammalian cells by antagonizing ER/Golgi SNAREs. Mol Biol Cell 21:1850–1863.

Unni VK, Weissman TA, Rockenstein E, Masliah E, McLean PJ, Hyman BT (2010) In vivo imaging of alpha-synuclein in mouse cortex demonstrates stable expression and differential subcellular compartment mobility. PLoS One 5:e10589.

van Ham TJ, Thijssen KL, Breitling R, Hofstra RM, Plasterk RH, Nollen EA (2008) *C. elegans* model identifies genetic modifiers of alpha-synuclein inclusion formation during aging. PLoS Genet 4:e1000027.

Waites CL, Leal-Ortiz SA, Andlauer TF, Sigrist SJ, Garner CC (2011) Piccolo regulates the dynamic assembly of presynaptic F-actin. J Neurosci 31:14250–14263.

Willingham S, Outeiro TF, DeVit MJ, Lindquist SL, Muchowski PJ (2003) Yeast genes that enhance the toxicity of a mutant huntingtin fragment or alpha-synuclein. Science 302:1769–1772.